TARGET ENUMERATION IN SENSOR NETWORKS VIA INTEGRATION WITH RESPECT TO EULER CHARACTERISTIC *

YULIY BARYSHNIKOV † AND ROBERT GHRIST ‡

Abstract. We solve the problem of counting the total number of observable targets (*e.g.*, persons, vehicles, etc.) in a region based on local counts performed by a network of sensors, each of which measures the number of targets nearby but not their identities nor any positional information. We formulate several such problems based on the types of sensors and mobility of the targets. The main contribution of this paper is the adaptation of a topological integration theory — integration with respect to Euler characteristic — to yield complete solutions to these problems.

1. Introduction. The prospect of small-scale sensor devices comes with the promise of sensor networks which can survey a region with a continuum-like coverage [8]. With this promise, however, comes many challenges, including power consumption, heat dissipation, and communication complexity. One strategy for remedying the situation is to focus on *minimal* sensing — engineering the individual sensors to be as simple as possible to accomplish the task and thus consume a minimum of resources.

We consider how to solve a simple global problem — counting targets — with a large array of local sensors which are as simple as possible. Specifically, we show that one can solve enumeration problems with sensors that can count nearby targets but cannot determine target identities, cannot estimate target range or bearing, and cannot record a time when a (moving) target came into view. Because the local sensors we envisage cannot discriminate targets, it is not possible to merge redundant counting by neighboring nodes. We present several mathematical formulations of this problem, varying the types of sensors used, the time-dependent features of the sensor nodes, and the time-dependent features of the observables.

It may seem surprising that a redundant array of simplistic sensors can solve the global enumeration problem. More surprising still is the fact that there are very few requirements on the sensors' detection specifications. We do not require that target visibility is purely a function of distance (cf. the typical use of the *unit disc* assumption in coverage problems). There are no hidden assumptions about convexity of the targets' detection zones, nor that the sensors or targets are uniform: some targets may be more 'visible' than others.

The reason for this combination of extreme robustness and extreme simplicity of the sensor capabilities is the nature of our solution methods. We use a topological invariant — the *Euler characteristic* — molded into an appropriate integration theory.

1.1. Problem statements. All of the problems in the list to follow involve determining a global count based on a local count. We are motivated by enumeration problems in sensor networks and thus present a number of scenarios based on different sensor modalities and system features.

*This work supported by DARPA # HR0011-07-1-0002.

† Mathematical and Algorithmic Sciences, Bell Laboratories, Murray Hill NJ, USA. *email:* ymb@research.bell-labs.com

‡ Department of Mathematics and Coordinated Sciences Laboratory, University of Illinois, Urbana IL, USA. *email:* ghrist@math.uiuc.edu

PROBLEM 1.1. **Counting fixed targets.** Let X denote a topological space. Referred to as the WORKSPACE, X is in practice some domain in either $\mathbb{R}^2$ or $\mathbb{R}^3$. Assume there is a finite number of observables $\mathcal{O}_\alpha$ in X and to each observable is associated a SUPPORT, U_α, a compact contractible subset in the workspace X. This support represents the set of sensor locations from which $\mathcal{O}_\alpha$ is "visible." Assume a sensor modality in which each node $x \in \mathcal{N}$ records the number of observables in range. This yields a HEIGHT FUNCTION,

$$h(x) := \#\{\alpha \,:\, x \in U_\alpha\}, \tag{1.1}$$

and represents the 'count' that a collection of sensors on X gives of the targets $\mathcal{U}$: see Fig. 3.1. The problem is to compute $|\mathcal{U}|$, the number of elements of $\mathcal{U}$, given only the height function h.

PROBLEM 1.2. **Counting wave fronts.** Another application is as follows. Consider a finite collection of points $\mathcal{O}_\alpha$ in $\mathbb{R}^n$, representing an event which occurs at some time and which triggers a wavefront that propagates for a finite time/extent before dissipating: see Fig. 1.1[left]. Assume that each sensor has the ability to record the presence of a wavefront which passes through its vicinity. Nodes have a simple counter memory which allows them to track the number of wavefronts they have experienced, but neither the time nor the direction/speed of the front. The event location $\mathcal{O}_\alpha$ along with the union of all its wavefronts is assumed to yield a contractible set U_α which represents the time-independent support of the event. Under these assumptions, the sensor wavefront counts correspond precisely to the height function of Eqn. (1.1).

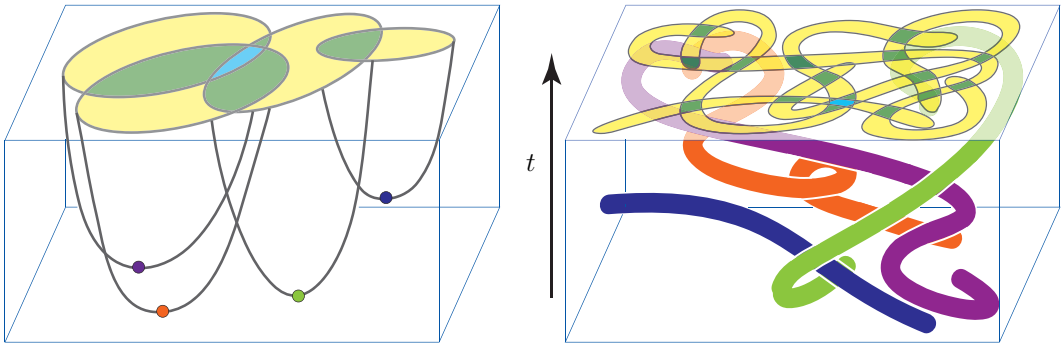

FIG. 1.1. *Two examples of time-dependent enumeration problems in the plane: [left] propagating wavefronts and [right] moving observables. In both cases, the sensor nodes are fixed and count via incrementing and internal counter.*

PROBLEM 1.3. **Counting motion paths.** In this setting, one has a finite collection of observables $\mathcal{O}_\alpha$ which move along continuous paths $\mathcal{O}_\alpha(t)$ in the domain, see 1.1[right]. Assume that sensor nodes can detect when some observable comes within proximity range (a time-dependent support $U_\alpha(t)$ which is contractible for each t), and that each such detection produces an increment in its internal counter: such increments occur only when the node detects an increase in the number of observables within range. One obtains a height function h of the form:

$$h(x) := \#\left\{(t,\alpha) \,:\, x \in U_\alpha(t+\epsilon) \text{ and } x \notin U_\alpha(t-\epsilon) \text{ for } \epsilon \to 0\right\} \tag{1.2}$$

One interesting feature in this setting is the possibility that the TRACE of the path $\mathcal{O}_\alpha(t)$ — the union of supports $\cup_t U_\alpha(t)$ — can be a non-contractible set, as in Fig. 3.3.

1.2. Statement of results. Our contributions consist of the following.

1. We prove that the number of elements in the collection, $|\mathcal{U}|$, is equal to the integral of the height function h with respect to the Euler characteristic measure.
2. We demonstrate that this integral may be computed in several ways: in terms of level sets, in terms of upper excursion sets, or in terms of a Morse theory for critical cells.
3. We give conditions under which the integral for $|\mathcal{U}|$ can be computed exactly when the height function h is known only on a network of discrete points.
4. We give heuristic methods for estimating $|\mathcal{U}|$ via integrals when h is sampled over a sparse network.
5. We catalogue a number of singular defects that can appear in the height function for various sensor modalities, with corresponding impacts on the Euler characteristic integrals.

We begin in §2.1 with the basic results from integration with respect to Euler characteristic, establishing points (1) and (2) above in §2-4. Examples follow in §3. In §5 we consider enumeration based on network data and work towards (3) through (5) above. The three problems in §1.1 are solved explicitly, along with an additional problem in §5.3.3 about sensors which perform a rotational 'sweep' of their surroundings.

Although our applications are novel, all of the mathematical tools used in this paper are well-known and fairly elementary. Specifically, we use the the following techniques.

1. **Integration with respect to Euler characteristic:** These methods, invented by Viro [25] and Schapira [21] independently, are a simple analytic interpretation of the classical Euler characteristic. These methods ultimately derive from sheaf theory [15, 22].
2. **Morse theory:** This classical theory dates back almost a century and provides a link between topological and analytic properties of functions. See, e.g., [19] for a treatment of the classical theory and [9] for a more modern approach applicable to the (degenerate) functions arising in this paper.

Morse theory is a fundamental tool in modern mathematics and lies at the root of applications across numerous scientific and engineering disciplines. In contrast, integration with respect to Euler characteristic is known mostly to mathematicians, though see [22] for an application to tomography, as well as [16] for recent work on using Euler characteristic integrals to compute volumes. Integrals involving Euler characteristic appear frequently in the literature on integral geometry (going back to works of Blaschke [3] and Hadwiger [12]) and convex geometry [10, 20]. More recently, integrals involving Euler characteristic have arisen in analyses of the geometry of Gaussian random fields, as in [1, 2, 26, 27, 23]. Many of these papers appear to use integration with respect to Euler characteristic without the formal machinery.

We are not aware of any similar approaches to problems in target estimation or tracking, the literature on which seems to always assume the ability to identify different targets (along with other high-level functions, including distance estimation, bearing estimation, and sensor localization). For example, the large-scale wireless system implemented in [13] assumes an aggregation phase based on strict spatial separation of targets. Jung and Sukhatme [14] implement a multi-target robotic tracking system where the targets are labeled with colored lights. The survey paper of Guibas [11] and the broader literature on geometric range-searching assumes the ability to aggregate target identities and concerns itself with

computational complexity issues. The paper by Li *et al.* [18] on multi-target tracking via sensor networks notes that, *"target classification is arguably the most challenging signal processing task in the context of sensor networks."*

We circumvent the complexities of target identification in the global counting problems of this paper by adopting the perspective of *minimal sensing*, in which the sensor nodes are assumed to be extremely simple with minimal capabilities. We are not aware of any other solutions to this enumeration problem which use nothing more than local sensor node counts without geometric data about the target identity, distance, or bearing.

That being said, we have ignored for the moment many of the important technical issues associated with network implementation of our methods. Much of the work in aggregation of data by a network concerns network protocols for signal processing [18], managing constraints on bandwidth and energy [4], and dealing with errors or node failures [28]. This introductory paper does not treat these important issues.

2. Counting via Euler characteristic integration.

2.1. The Euler characteristic integral. Our results follow from the classical and elegant theory of integration with respect to Euler characteristic [25, 21]. Recall that the Euler characteristic of a compact cell (simplicial, CW, or other) complex A is equal to the alternating sum of the number of cells, graded by dimension; or, more generally, by the alternating sum of the ranks of the homology groups $H_k(A)$:

$$\chi(A) := \sum_{k=0}^{\infty} (-1)^k \dim(H_k(A)) = \sum_{k=0}^{\infty} (-1)^k \#\{k\text{-cells in } A\}. \tag{2.1}$$

The Euler characteristic is defined only on those sets for which the sum above converges. See, *e.g.*, [24] for more information on classes of spaces for which χ is well-defined. In applications relevant to this paper, all sets will be piecewise real-analytic, leading to no complications about well-definedness of χ.

EXAMPLE 2.1. Euler characteristic is a generalization of cardinality: for a finite point set A, $\chi(A) = |A|$. More generally, if A is a compact contractible set — if it can be deformed continuously within itself to a single point — then $\chi(A) = 1$. For a compact topological graph Γ, the Euler characteristic is $\chi(\Gamma) = \#V(\Gamma) - \#E(\Gamma)$. Finally, if $A \subset \mathbb{R}^2$ is a compact connected domain with N holes, then the Euler characteristic is $\chi(A) = 1 - N$.

The subadditivity property of the Euler characteristic $\chi(A \cup B) = \chi(A) + \chi(B) - \chi(A \cap B)$ on compact sets allows one to interpret it as a generalized measure (it is finitely additive and can take on negative values). One can check that as long as no measure-theoretical issues arise, the measure behaves in exactly the same way as any conventional measure. This leads to a standing assumption of finiteness of all sums and unions of elements in the collection of sets. More formally:

DEFINITION 2.2. *A collection $\mathcal{A}$ of subsets of a topological space X is said to be* TAME *if $\mathcal{A}$ is closed with respect to the operations of finite intersection, finite union and complement, and all elements of $\mathcal{A}$ possess well-defined Euler characteristics.*

We will sometimes abuse the notation and call a collection tame if its closure under finite intersection, finite union, and complement satisfies Definition 2.2.

DEFINITION 2.3. *Let $\mathcal{A}$ be a tame collection of compact subsets of X. Choose a commutative coefficient ring R and let $\phi = \sum \lambda_\alpha \mathbb{1}_{U_\alpha}$ be a finite R-linear combination of indicator functions of elements $U_\alpha \in \mathcal{A}$. The* INTEGRAL *of ϕ with respect to Euler characteristic is defined to be*

$$\int_X \phi \, d\chi := \sum_\alpha \lambda_\alpha \chi(U_\alpha). \tag{2.2}$$

It follows easily from the fact that $\chi(A \cup B) = \chi(A) + \chi(B) - \chi(A \cap B)$ that this integral is well-defined:

LEMMA 2.4 ([25, 21]). *Let $\mathcal{A}$ be a tame collection and $\phi = \sum \lambda_\alpha \mathbb{1}_{U_\alpha}$ a finite R-linear combination of indicator functions of elements $U_\alpha \in \mathcal{A}$. Then $\int \phi \, d\chi$ depends only on the function ϕ and not on the decomposition.*

A Fubini-type theorem is valid. Consider a continuous map $F : X \to Y$ with algebras of tame sets $\mathcal{A}_X$ and $\mathcal{A}_Y$. One says that F is TAME if, roughly speaking, inverse images of F are well-behaved with respect to $\mathcal{A}_X$.[1] In the class of piecewise-linear or real-analytic settings, tameness is always satisfied: see [5, 24] for a detailed treatment.

THEOREM 2.5 (Fubini Theorem [25, 21]). *Let $F : X \to Y$ be a tame mapping with $h : X \to R$ a compatible tame function. Then*

$$\int_X h(x) \, d\chi(x) = \int_Y \left(\int_{F^{-1}(y)} h(x) \, d\chi(x) \right) d\chi(y). \tag{2.3}$$

A great deal more is true about integration with respect to χ: see, *e.g.*, [25, 21, 5, 6] for a sampling.

2.2. Enumeration and integration. Lemma 2.4 immediately yields a solution to Problem 1.1 of §1.1, assuming a complete description of the height function over the entire cell structure.

THEOREM 2.6. *Given $\mathcal{U} = \{U_\alpha\}$ a tame collection of compact contractible subsets of a topological space X and $h : X \to \mathbb{N}$ the height function $h(x) = \#\{\alpha : x \in U_\alpha\}$, the cardinality of $\mathcal{U}$ is equal to*

$$|\mathcal{U}| = \int_X h \, d\chi. \tag{2.4}$$

Proof. The height function h is the sum of indicator functions $h = \sum_\alpha \mathbb{1}_{U_\alpha}$. Since each U_α is contractible, $\chi(U_\alpha) = 1$ and $\int_X h \, d\chi = \sum_\alpha 1 = |\mathcal{U}|$. □

This result (formally) solves Problem 1.1 as well as to Problems 1.2 and 1.3 when the time-aggregated supports are contractible sets (*e.g.*, the traces are non-self-intersecting). In the case of time-dependent support sets whose trace in X has 'tame' self-intersections, one requires the following extension of the result.

[1] Specifically, (1) $F^{-1}(y) \in \mathcal{A}_X$ for all $y \in Y$; and (2) for any $U \in \mathcal{A}_X$, there exists a filtration $V_0 \subset V_1 \subset \dots$ with $V_i \in \mathcal{A}_Y$ and the projection $F : F^{-1}(V_i - V_{i-1}) \cap U \to V_i - V_{i-1}$ is a locally trivial (Serre) fibration [25].

Consider a collection of compact contractible spaces $\{U_\alpha\}$ and let $F : \coprod_\alpha U_\alpha \to X$ be a continuous map from the disjoint union into a topological space X. For example, in the setting of Theorem 2.6, F restricted to each U_α is an inclusion map into X. The appropriate height function in this setting is that which counts the number of connected components of the inverse images $\{F^{-1}(x)\}$ in the disjoint union.

THEOREM 2.7. *Consider $\mathcal{U} = \{U_\alpha\}$ a collection of compact contractible spaces and a tame map $F : \coprod U_\alpha \to X$ to a topological space X. Then the cardinality of $\mathcal{U}$ is equal to $|\mathcal{U}| = \int_X h\, d\chi$, where $h : X \to \mathbb{N}$ is the height function*

$$h(x) = \chi\left(F^{-1}(x)\right). \tag{2.5}$$

Proof. Let $U := \coprod_\alpha U_\alpha$, and apply the Fubini theorem to the integral of $\mathbb{1}_U$ via the map F:

$$|\mathcal{U}| = \int_U \mathbb{1}_U\, d\chi = \int_X \left(\int_{F^{-1}(x)} \mathbb{1}_U\, d\chi \right) d\chi = \int_X h\, d\chi. \tag{2.6}$$

□

The height function of Eqn. (2.5) is precisely that returned by a sensor which counts the number of times that an observable changes from a non-proximate state to a proximate state: cf. Problem 1.3. In this setting, $\chi(F^{-1}(x))$ is equal to the total number of connected components of the sets in all the U_α which are sent to x — that is, the number of times that the sensor node at x 'sees' some observable.

2.3. Computation. There are several direct and to various degrees intuitive ways to compute this integral. Two are immediate.

THEOREM 2.8. *Given a height function $h : X \to \mathbb{N}$, the integral of h with respect to $d\chi$ may be computed as follows:*

$$\int_X h\, d\chi = \sum_{s=0}^{\infty} s \cdot \chi\left(h^{-1}(s)\right) \tag{2.7}$$

$$= \sum_{s=0}^{\infty} \chi\left(h^{-1}((s,\infty))\right) \ . \tag{2.8}$$

Proof. Both equations follow from Lemma 2.4, by integrating the function $h(x)$ with respect to Lebesgue measure in different ways. Eqn. (2.7) follows from rewriting $\sum_\alpha \mathbb{1}_{U_\alpha}$ via the 'shell method' of integration, and Eqn. (2.8) follows from the 'disc method' of integration. □

It will be important for applications to sensor networks to integrate real-valued functions with respect to Euler characteristic. The usual limiting process extends Definition 2.3 from finite Riemann sums to integrable limits.

REMARK 2.9. In the case of a height function $h : X \to [0,\infty)$, the formulæ of Theorem 2.8 become:

$$|\mathcal{U}| = \int_{s=0}^{\infty} s \cdot \chi\left(h^{-1}(s)\right)\, ds = \int_{s=0}^{\infty} \chi\left(h^{-1}((s,\infty))\right)\, ds. \tag{2.9}$$

3. Examples. Theorem 2.8 makes it very easy to compute $|\mathcal{U}|$.

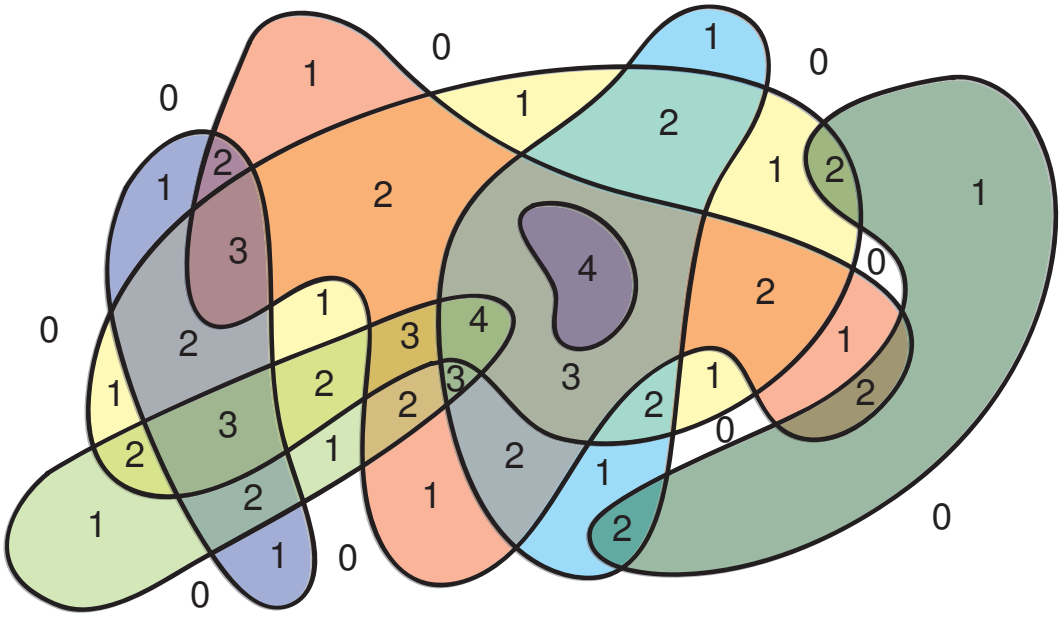

FIG. 3.1. *A collection of contractible patches $\mathcal{U} = \{U_\alpha\}$ in $\mathbb{R}^2$ corresponding to the supports or 'visibility regions' of seven targets. The collection $\mathcal{U}$ decomposes $\mathbb{R}^2$ into cells labeled according to the height function h returned by a dense sensor network.*

EXAMPLE 3.1. In the example of Fig. 3.1, seven contractible sets $\mathcal{U}$ are displayed, along with a height function on connected components. In the intended application, only h is known, not $\mathcal{U}$. Decomposing h into upper excursion sets (Fig. 3.2) allows one to compute $\int h\, d\chi$ via Eqn. (2.8):

$$\int h\, d\chi = \sum_{s=0}^{\infty} \chi\left(h^{-1}((s,\infty))\right) = \overbrace{2}^{s=3} + \overbrace{3}^{s=2} + \overbrace{3}^{s=1} + \overbrace{-1}^{s=0} = 7. \tag{3.1}$$

We note that it is preferable to compute χ-integrals via upper excursion sets, Eqn. (2.8), as opposed to level sets, Eqn. (2.7). The levels sets of h in Fig. 3.2 are 'fragile' in the sense that removing an small ϵ-neighborhood of the boundary of $h^{-1}(s)$ usually changes the topology (and hence the Euler characteristic) of the level set. The upper excursion sets are less likely to exhibit such behavior.

EXAMPLE 3.2. Fig. 3.3 illustrates a height function associated to a moving-target situation as in Problem 1.3, in which one wants to count the number of paths traced out in a domain, in this case $\mathbb{R}^2$. Note that some traces self-intersect. Invoking Theorem 2.7, one computes:

$$\int h\, d\chi = \sum_{s=0}^{\infty} \chi\left(h^{-1}((s,\infty))\right) = \overbrace{1}^{s=3} + \overbrace{9}^{s=2} + \overbrace{28}^{s=1} + \overbrace{-31}^{s=0} = 7. \tag{3.2}$$

This final count is not obvious from inspection as it is in Fig. 3.1.

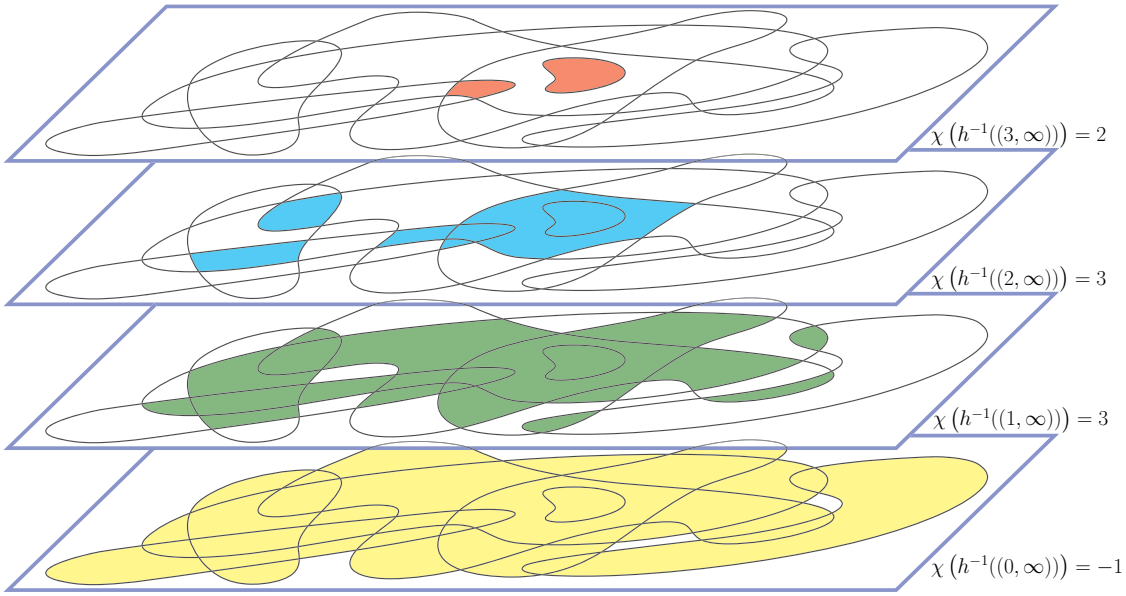

FIG. 3.2. *Decomposing h into upper excursion sets and computing χ yields the integral $\int h\, d\chi$.*

4. Morse theory. We relate the integral of h with respect to Euler characteristic to an index-weighted sum of critical values of h (properly interpreted). This is a localization result, reducing from an integral over all of X to an integral over a (small) set of critical cells/points. We assume a passing familiarity with basic Morse theory: see [19] for a more detailed introduction.

4.1. Smooth Morse functions. We begin with a simple treatment of integration of a smooth Morse function with respect to Euler characteristic. Recall that a real-valued function $f : M \to \mathbb{R}$ on a smooth manifold M is MORSE if all critical points of f are nondegenerate, in the sense of having a nondegenerate Hessian matrix of second partial derivatives. Denote by $\mathcal{C}(f)$ the set of critical points of f. For each $p \in \mathcal{C}(f)$, the MORSE INDEX of p, $\mu(p)$, is defined as the number of negative eigenvalues of the Hessian at p, or, equivalently, the dimension of the unstable manifold of the vector field $-\nabla f$ at p.

LEMMA 4.1. *If f is a Morse function on an n-dimensional manifold M, then*

$$\int_M f\, d\chi = \sum_{p \in \mathcal{C}(f)} (-1)^{n-\mu(p)} f(p). \tag{4.1}$$

Proof. Assume first that all critical values are distinct. The Euler characteristic of level sets and excursion sets is piecewise-constant, changing only at critical values. For $p \in \mathcal{C}(f)$, $s = f(p)$, and $\epsilon \ll 1$, elementary Morse theory [19] says that $f^{-1}(-\infty, s+\epsilon)$ differs from $f^{-1}(-\infty, s-\epsilon)$ by the addition of a HANDLE — a product of discs $D^{\mu(p)} \times D^{n-\mu(p)}$ glued along $\partial D^{\mu(p)} \times D^{n-\mu(p)}$. The change in Euler characteristic resulting from this handle addition is $(-1)^{\mu(p)}$. From this it follows that

$$\chi(f^{-1}(s+\epsilon, \infty)) - \chi(f^{-1}(s-\epsilon, \infty)) = (-1)^{n-\mu(p)}. \tag{4.2}$$

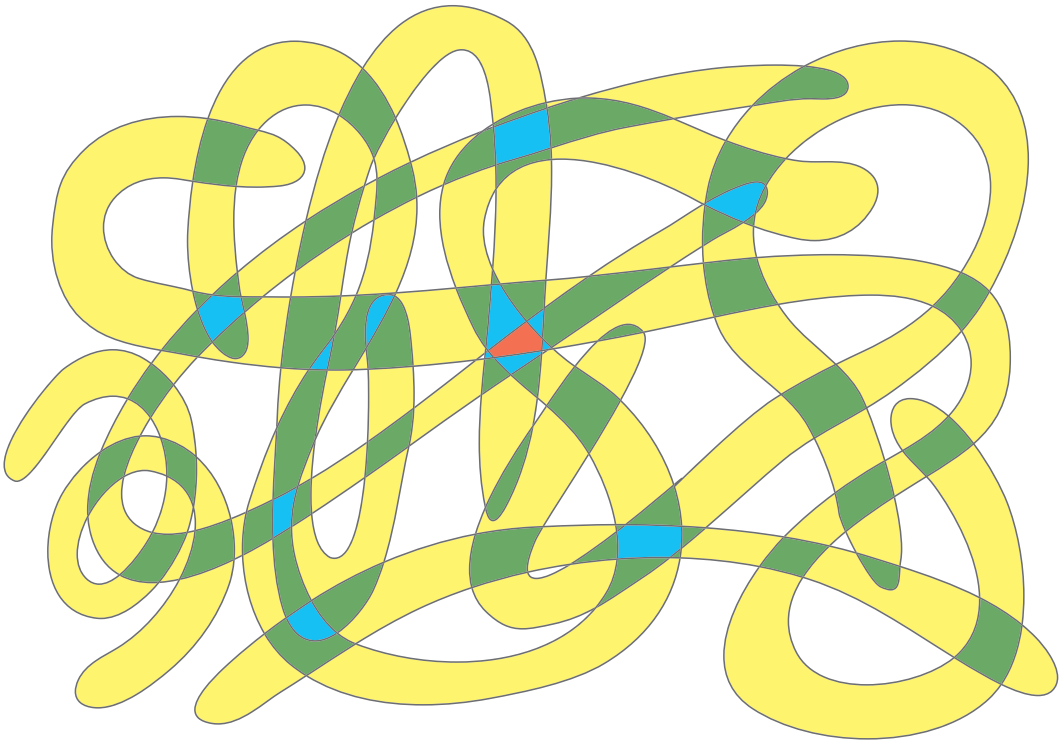

FIG. 3.3. *Vehicles moving in a planar environment activate sensors along regions which intersect over time and accumulate a larger height function there.*

Eqn. (2.8) combined with the above yields

$$\int_M f\, d\chi = \int_0^\infty \chi(f^{-1}(s,\infty))ds = \sum_{p\in\mathcal{C}(f)} (-1)^{n-\mu(p)} f(p). \tag{4.3}$$

If f does not have distinct critical values, the subadditivity of χ and of the integral yield the same result. □

Thus, there is a great deal of variability permitted within f; the χ-integral is determined by the critical set. As a simple example, the following is immediate from Lemma 4.1.

COROLLARY 4.2. *If M is a 1-dimensional manifold, $\int_M f\, d\chi$ is equal to half the total variation of f.*

4.2. Piecewise-constant height functions. In the context of a continuous 'field' of sensors, the height function h is piecewise-constant and by no means Morse. However, the argument of Lemma 4.1 generalizes directly. The Morse theory simplifies under a regularity assumption for the collection $\mathcal{U}$. For the remainder of this section, assume the following:

ASSUMPTION 4.3. *For any subset $I \in \mathcal{A}$, the intersection $U_I := \cap_{\alpha\in I} U_\alpha$ is the closure of the intersection of the interiors of $U_\alpha, \alpha \in I$, In particular, the sets U_α themselves have that property.*

Such an boolean algebra of sets will be referred to as REGULAR. A regular collection $\mathcal{U}$

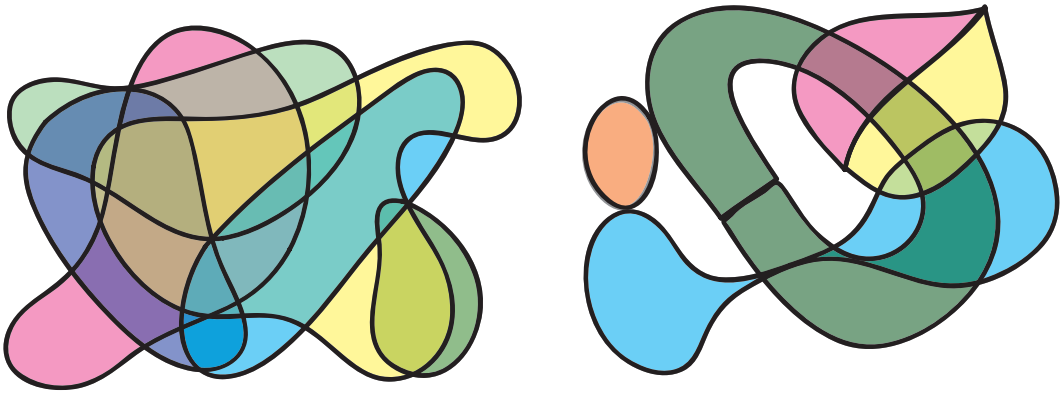

FIG. 4.1. *Examples of regular [left] and nonregular [right] collections of contractible sets in* $\mathbb{R}^2$.

divides the ambient space X into well-defined cells or CHAMBERS — closures of the connected components of the interior of a level set of h. Under the assumption of regularity, the upper excursion sets $h^{-1}((s,\infty))$ are a union of chambers glued together along those portions of their boundaries where h increases upon exiting the chamber. The following definitions are standard in many variants of Morse theory (degenerate Morse theory, Gromoll-Meyer pairs, and Conley index theory being prime examples).

DEFINITION 4.4. *A chamber V for a regular height function h is* CRITICAL *if the Euler characteristic of V differs from the Euler characteristic of the* EXIT SET *of V, $V^+ := \{p \in \partial V \,:\, h(p) \geq h(V)\}$. The* INDEX *of the chamber, $\mathcal{I}_V := \chi(V, V^+) = \chi(V) - \chi(V^+)$ is thus nonzero iff V is critical. Denote by $\mathcal{C}(h)$ the set of critical chambers of h.*

Invoking subadditivity, one concludes that $\int h\, d\chi$ is the sum of values of h weighted by the Euler characteristics of the chambers, with boundary overlaps subtracted. The following result localizes the χ-integral to the critical chambers, and is a cellular analogue of Lemma 4.1.

THEOREM 4.5. *For $h : X \to \mathbb{N}$ a regular height function on X,*

$$\int_X h\, d\chi = \sum_V \mathcal{I}_V h(V) = \sum_{V \in \mathcal{C}(h)} \mathcal{I}_V h(V). \tag{4.4}$$

Proof. This follows directly from Definition 4.4, the subadditivity of the Euler characteristic, and Eqn. (2.8). □

In most cases, $\mathcal{I}_V = (-1)^k$ for k corresponding to the Morse co-index of the chamber: cf. Lemma 4.1.

EXAMPLE 4.6. The collection $\mathcal{U}$ from Example 3.1 gives a regular partition of the plane

with critical chambers shaded in Fig. 4.2. Using Eqn. (4.4) we compute:

$$\begin{aligned}\int h\, d\chi &= \sum_{V\in\mathcal{C}(h)} \mathcal{I}_V h(V) \\ &= 4(\overbrace{1+1}^{h^{-1}(4)}) + 3(\overbrace{1+1-1}^{h^{-1}(3)}) + 2(\overbrace{1+1+1-1-1-1}^{h^{-1}(2)}) + 1(\overbrace{1-1-1-1-2}^{h^{-1}(1)}) \\ &= 7\end{aligned}$$

.

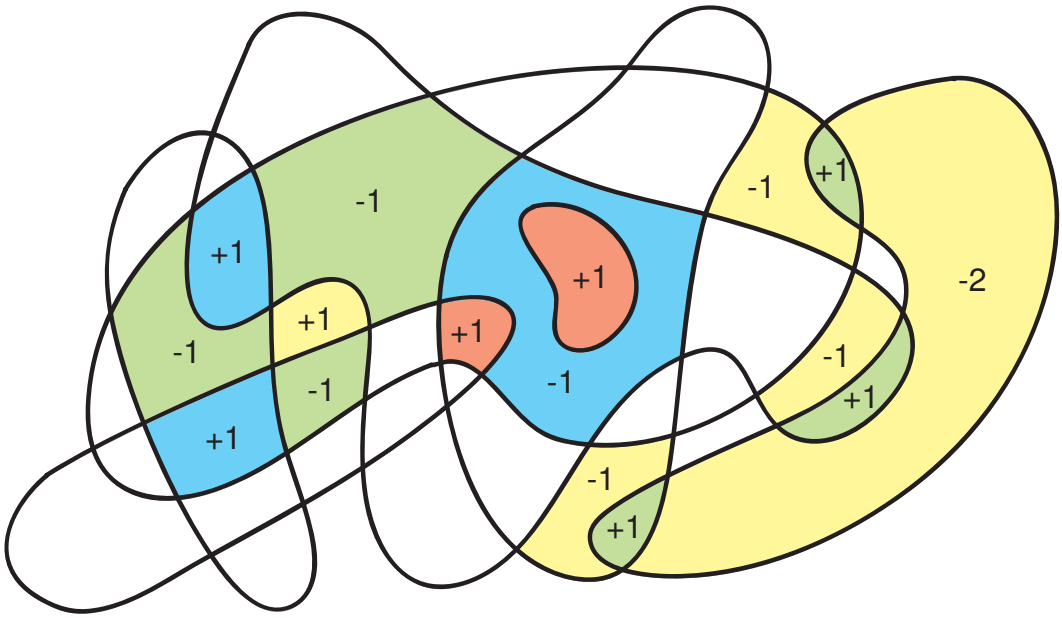

FIG. 4.2. *The collection $\mathcal{U}$ from Example 3.1 yields a regular partition of the plane. Critical chambers with non-zero h-values are shaded and labeled according to index $\mathcal{I}$.*

5. Applications to networks. The motivation for this work is to enumerate observables based on data from a sensor network. We have developed the integration theory appropriate to solving the problem given a continuum field of sensors. In practice, however, one receives a sampling of the height function h on a discrete subset of nodes $\mathcal{N} \subset X$. Such a sampling may or may not be fine enough to determine the true count. However, since the true count is represented as an integral, we can use intuitions from numerical integration to estimate $\int_X h\, d\chi$.

5.1. Piecewise-linear height functions. Assume for the remainder of this section that the domain X is Euclidean n-dimensional space and that $\mathcal{N} \subset \mathbb{R}^n$ is the vertex set of a grid on which h is sampled. The grid may be regular (*e.g.*, square or hexagonal in 2-d) or irregular (*e.g.*, the Delaunay triangulation of a sampling of points). We claim that the best approach for enumerating observables based on a point sampling is to work not in the class of piecewise-constant height functions, but rather with piecewise-linear (PL) interpolations. The appropriate PL interpolation depends on the geometry of the grid.

Assume for simplicity that the given grid on $\mathcal{N}$ is a triangulation $T_{\mathcal{N}}$, so that the PL interpolation $\bar{h}$ of the height function is well-defined.

QUESTION 5.1. Under what circumstances does the integral $\int \bar{h}\, d\chi$ give a correct count of $|\mathcal{U}|$?

The hope for this estimate derives from the Morse results of §4. Recall that $\int h\, d\chi$ is determined by its values on critical cells (Theorem 4.5), just as $\int \bar{h}\, d\chi$ is determined by its values on critical points (Lemma 4.1). Thus, if the sampling of h is faithful enough so that $\bar{h}$ captures the critical point set of h, then the integrals with respect to χ will agree. This is the basis of the following.

THEOREM 5.2. *Let $\mathcal{U} = \{U_\alpha\}$ denote a collection of compact contractible sets in $X \subset \mathbb{R}^n$ whose boundaries $\{\partial U_\alpha\}$ are each C^1 hypersurfaces and collectively in general position, so that the tangent cones defined at intersection points of the hypersurfaces have angles bounded below by a constant $C_a > 0$. Assume that $T_{\mathcal{N}}$ is a triangulation of X satisfying the following.*

- *The mesh $T_{\mathcal{N}}$ is* BALANCED*: the spatial angles spanned by the simplices at the vertices are bounded from below by a uniform constant C_t.*
- *The mesh $T_{\mathcal{N}}$ is* FINE*: the diameters of all simplices are less than $K(n, C_a, C_t)$, where K is a universal function depending on the dimension and the conditioning constants C_h and C_t.*

Then $|\mathcal{U}| = \int \bar{h}\, d\chi$.

Proof. We provide a sketch. The condition on the diameters of $T_{\mathcal{N}}$ implies that $\mathcal{N}$ has an element (a witness) in each of the sets

$$\left(\bigcap_{\alpha\in I} U_\alpha\right) \cap \left(\bigcap_{\beta\in J} X - U_\beta\right), \tag{5.1}$$

for all I and J such that the intersection is non-empty.

The proof of the theorem follows by constructing a joint homotopy of the sets $\mathcal{U}$ on the subcomplexes of the triangulation $T_{\mathcal{N}}$. We sketch the construction of the homotopies, refraining from (customarily tedious) details. As each border hypersurface ∂U_α is smooth, one can define a function λ_α nondegenerate in some vicinity of ∂U_α. Furthermore, as the border hypersurfaces intersect transversally, the functions $\{\lambda_\alpha\}, \alpha \in I$ define a (perhaps, incomplete) coordinate system near the intersection manifold $\cap_{\alpha\in I}\partial U_\alpha$. In other words, we choose local charts near the border hypersurfaces in such a way that the functions locally defining these hypersurfaces become linear.

As the simplices of the original triangulation are small and balanced, $T_{\mathcal{N}}$ can be homotopically straightened near the border hypersurfaces, so that the functions λ_α become linear on these deformed simplices. Let $\tilde{h}$ be the PL continuation of the height function $h|_{\mathcal{N}}$ from $\mathcal{N}$ to this deformed triangulation. The fact that on the simplices where $\tilde{h}$ is non-constant it is linear implies that all supersets $\{h \geq s\}$ can be retracted to the union of simplices of $T_{\mathcal{N}}$ spanning the vertices of $\mathcal{N}$ where $h \geq s$. □

EXAMPLE 5.3. Fig. 5.1 gives an example of a collection $\mathcal{U}$ with height function sampled on a uniform hexagonal grid. The upper excursion sets of the PL interpolation $\bar{h}$ are easily

computed. The integral of $\bar{h}$ with respect to Euler characteristic is thus:

$$|\mathcal{U}| = \int \bar{h}\, d\chi = \overbrace{1}^{s=3} + \overbrace{3}^{s=2} + \overbrace{0}^{s=1} = 4. \tag{5.2}$$

It is clear from this example that the integral of $\bar{h}$ can return an accurate count, even when the collection $\mathcal{U}$ does not satisfy all the conditions of Theorem 5.2 — *e.g.*, the boundaries ∂U_α did not need to be C^1 in this example.

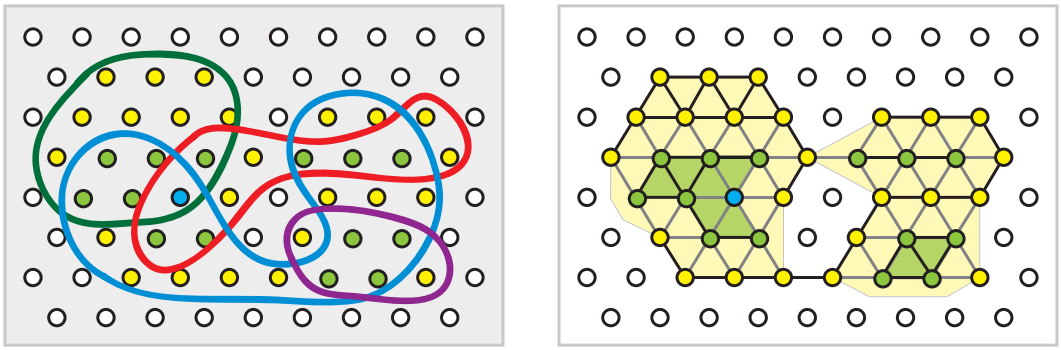

FIG. 5.1. *The height function of $\mathcal{U}$ sampled on a hexagonal grid [left] yields a PL interpolation whose upper excursion sets [right] accurately compute the integral with respect to Euler characteristic.*

REMARK 5.4. The condition of Theorem 5.2 on $\mathcal{U}$ is quite a bit stronger than that of Assumption 4.3. One glaring disadvantage of the construction above is that it starts with a fixed family $\mathcal{U}$ and derives from that the fine and balanced conditions on the triangulation needed to represent $\mathcal{U}$ faithfully. One way to overcome this disadvantage is to consider a generic *parametrized family* of sets (*e.g.*, up to small shifts); then one can estimate the size (*e.g.*, Lebesgue measure) of the set of parameters for which the construction above is not valid, in terms of the triangulations, the curvatures of the sets, and the cardinality of the collection.

5.2. Expected counts. In the previous subsection, the PL interpolation $\bar{h}$ was computed based on a triangulation of the domain. Because PL interpolations are uniquely defined on a simplex, there are no 'new' critical values in $\bar{h}$, and all critical values of $\bar{h}$ must be integers. However, when the grid for $\mathcal{N}$ is based on a more general cell decomposition, the correct interpolation $\bar{h}$ is not obvious, and, at the very least, can possess critical values at non-integer heights, with the corresponding integral having non-integer values. This represents not merely the ambiguity present in the construction of $\bar{h}$ but the ambiguity in the original sampling of h.

We claim (without proof of efficacy) that the appropriate strategy for a 'sparse' sampling of h over a cell structure which is not a triangulation is to create a PL interpolation $\bar{h}$ using auxiliary nodes obtained by averaging over the cell vertices (using weights based on the cell geometry). That the resulting integral $\int \bar{h}\, d\chi$ may have rational rather than integer values is then interpreted as an expected count which weighs the ambiguity in the sampling.

EXAMPLE 5.5. For a regular square grid, we augment $\mathcal{N}$ by adding an additional 0-simplex at the center of each square 2-cell and triangulating the 2-cells accordingly. This yields a natural PL height function $\bar{h}$ defined on the auxiliary nodes by averaging the four values

of h on the carrier square. The 2-d square grid of Fig. 5.2[left] has two nodes with $h = 1$ along the diagonal of a square cell; all other nodes return $h = 0$. With this sampling of h, it is uncertain whether the level set $h^{-1}(1)$ has Euler characteristic $+1$ or $+2$ — this is a manifestation of the *4-connect vs. 8-connect* problem in the "digital topology" of pixellated images [17]. In passing to the PL interpolation on the subdivided grid in Fig. 5.2[right], one checks that $\bar{h}$ has two maxima at $+1$ and a saddle point at height $\frac{1}{2}$ in the center of the square defined by the two maxima. Via the Morse-theoretic result in Lemma 4.1, we have $\int \bar{h}\, d\chi = 1 + 1 - \frac{1}{2} = \frac{3}{2}$. This is the *expected* count for $|\mathcal{U}|$. Without knowing more about the geometry of sensor or target supports, such an expected count for $|\mathcal{U}|$ is the best one can hope for.

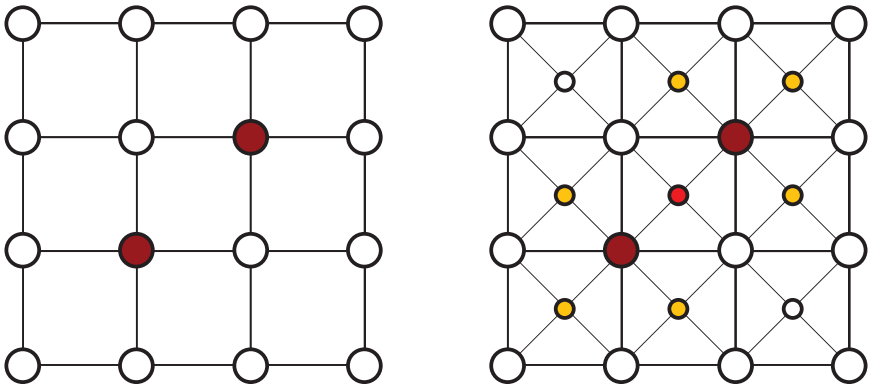

FIG. 5.2. *A height function sampled on a square grid [left] having two diagonal nodes at height $+1$ is refined to a PL height function $\bar{h}$ [right] which has two maxima at height $+1$ and a saddle at height $+\frac{1}{2}$. This yields $\int \bar{h}\, d\chi = \frac{3}{2}$, reflecting the ambiguity induced by the coarse sampling.*

In general, the interpolation of the height function should depend of the "granularity" of the sets $\mathcal{U}_\alpha$. A convenient setting for a rigorous analysis of such interpolations can be, conjecturally, obtained within the framework of stochastic geometry, *i.e.*, assuming the sets $\mathcal{U}_\alpha$ to be a random set process. In this case, the (necessarily linear) operator taking the restriction of the height function to the nodes incident to a cell, to the continuation of the function inside the cell, could be computed in terms of moments of the random bodies forming the set process.

In the case we considered above, where the scale of cells of the partition of X given by the nodes $\mathcal{N}$ is much smaller than the characteristic length of non-homogeneity of the sets $\mathcal{U}_\alpha$, the interpolation is in fact given by the largest concave minorant: if the cell C is a convex polytope and the values of h are fixed at the vertices, then the interpolation can be taken as the supremum over all (affine) linear function taking values at most h at all the vertices of the cell (see figure 5.3).

5.3. Defects. When estimating $|\mathcal{U}|$ via an integral, there are various types of defects that can arise in the integrands. For example, sensors may be subject to occasional errors in counting or to isolated node-failures, leading to a 'noisy' height function h. Such defects are independent of the system details. However, there are very specific types of defects which depend on the precise forms of sensors used and the problems solved. Here, we catalogue several classes of defects and their effects on the integrand. We leave for future work resolution of the claim that an appropriate form of averaging of the height function — an *annealing* — can smooth out the defects and lead to more accurate integrals.

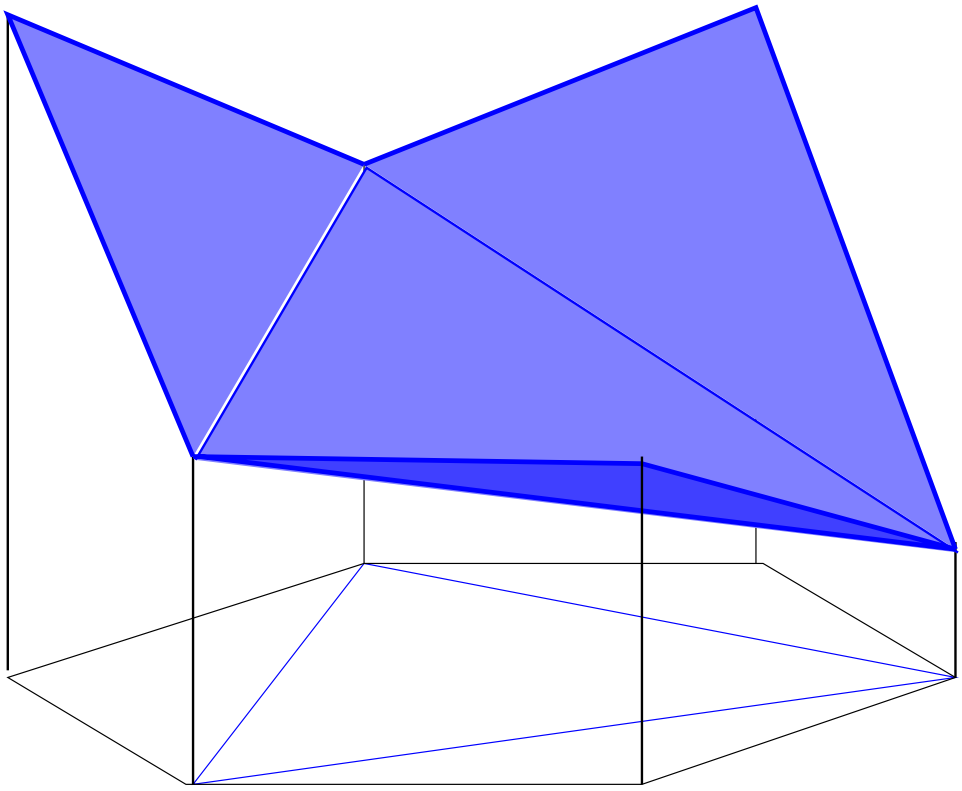

FIG. 5.3. *A minimal interpolation of the height function from the vertices of a hexagonal cell into its interior.*

5.3.1. Wavefront systems. In the sensor modalities of Problems 1.2 and 1.3, nodes increment an internal counter whenever an event (typically, a moving target) enters a node's detection range. One complication that can occur in practice is multiple targets coming into a node's range simultaneously. If the sensor is sufficiently coarse, it may register this as a single target detection, giving an inaccurate reading for h.

This is most likely to occur in the setting of Problem 1.2, where traveling wavefronts can overlap and propagate inaccurate readings, see Fig. 5.4[left]. For a continuous field of sensors, under the assumption that wavefronts are in general position, the set of simultaneous overlaps of n (mutually close) wavefronts traces out a stratified set of codimension $n-1$ in the domain. This immediately violates the regularity of the cell decomposition for h.

This problem can be readily overcome in this particular (idealized) setting by replacing the (precise) height function h by its upper-continuous approximation (the minimal upper continuous function majorizing h). Because these defects have strictly positive codimension, they are erased by this procedure.

5.3.2. Defects in counting tracks. In the context of path-counting as in Problem 1.3, there are different problems which can occur. Recall that in this sensor modality, an internal counter increments whenever the sensor changes state from *'no detection'* to *'detection.'* Sensors which base detection on perceived motion, as in the case of acoustic

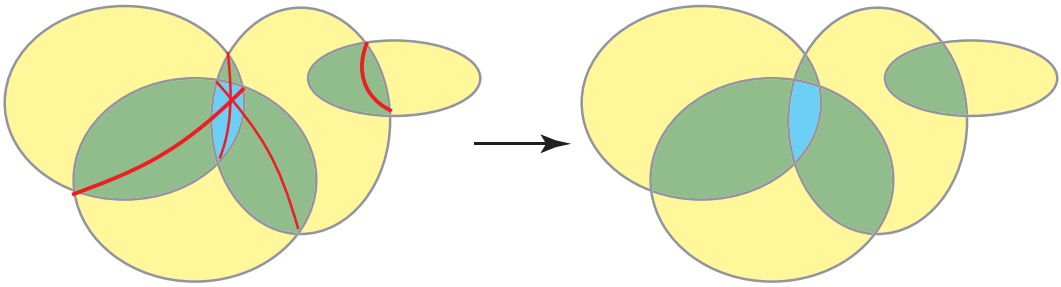

FIG. 5.4. *Propagating wavefronts may produce a height function which undercounts along the regions (curves [left]) in which wavefronts cross simultaneously. It is desirable to have a procedure which anneals the height function to remove these defects [right].*

sensors, can be 'tricked' into advancing their counter by a motion path which stops, waits, and then starts again. The Euler characteristic integral of the resulting height function will count the number of temporally distinct paths, which is not the desired goal of computing the number of targets. (Sensors which perform detection by means of proximity, *e.g.*, infrared sensors, will not present such a problem.)

No local annealing as in Fig. 5.4 will have the desired effect, since the defects here are codimension 0, and any relaxation strong enough to eliminate a (stop-start) local maximum on the 'interior' of a path would likely eliminate a valid local maximum on the intersection of two paths: see Fig. 5.5[left], which shows two targets leaving a sensor reading of three paths. This indicates that distinguishing start-stop paths via Euler characteristic integrals is difficult.

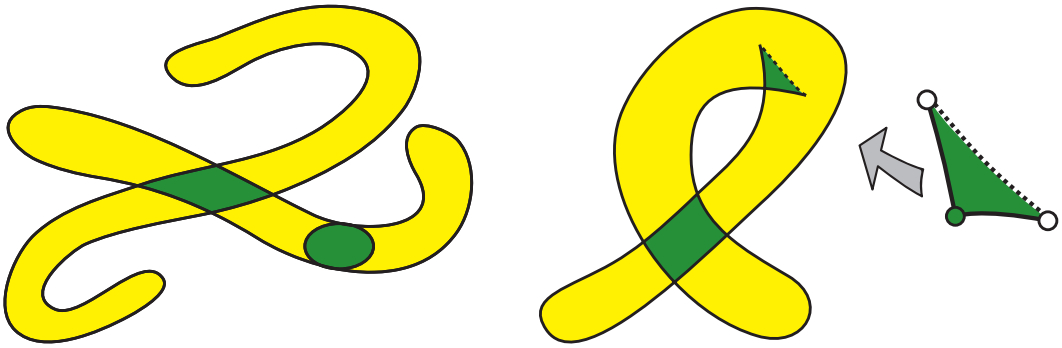

FIG. 5.5. *[left] Removing non-transverse local maxima within a path merges start-stop paths, but finding such may be difficult in a dense traffic zone and can miscount circular paths. Codimension-0 defects can also occur [center] when the temporal trace of target supports exhibits a local singularity. If one works in the category of non-closed cell complexes [right], the Euler integral still returns a valid answer.*

A more fundamental type of codimension-0 defect can occur, again based on properties of the projection from the space-time graph of the target traces down to the workspace. In all examples illustrated, we have assumed that the traces of the target supports do not admit any local singularities in the workspace projection. When such a singularity occurs, as in Fig. 5.5[center], there is a patch where h has a local maximum. This patch A, magnified in Fig. 5.5[right] is not compact, and has Euler characteristic equal to $\chi(A) = \chi(\bar{A}) - \chi(\bar{A} - A) = 1 - 1 = 0$. Thus, it does alter $\int h \, d\chi$, in accordance with Theorem 2.7.

However, any network sampling of this height function will not have fine details about ∂A and will erroneously compute $|\mathcal{U}|$.

5.3.3. Counting via sweeping sensors. The following is one of several possible examples of problems for which defects are inevitable.

PROBLEM 5.6. **Counting via sweeps.** Fix a Euclidean workspace $\mathbb{R}^n$ and consider a variant of Problem 1.1 in which sensor nodes do not return merely a count of the number of targets within range, but rather a parameterized count of targets as the sensor performs a 'sweep' over its visual sphere. For example, in $\mathbb{R}^2$, each sensor returns a piecewise-constant function $h_x : S^1 \to \mathbb{N}$ which indicates how many targets are seen as a function of bearing. Assume, for simplicity, that a sensor at location x with bearing $\boldsymbol{v} \in T^1_x(\mathbb{R}^n)$ scans a compact convex cone at x containing $\boldsymbol{v}$ that varies isometrically as a function of x and $\boldsymbol{v}$. The problem is how to compute $|\mathcal{U}|$ given the collection of functions $h = \{h_x : x \in X\}$, where $h_x(\boldsymbol{v})$ returns the number but not identity of targets within the cone at $(x, \boldsymbol{v})$.

For a very thin scanning cone, intersections with the targets never overlap, and $\chi(h_x^{-1}(1))$ yields the correct number of targets within range of x, reducing the problem to that of Problem 1.1. For more general cones, however, sweeping does not return an immediate count at x.

THEOREM 5.7. *Under the assumptions of Problem 5.6 and a general-position assumption on the targets $\{O_\alpha\}$, the number of targets is equal to*

$$\int_{\mathbb{R}^n} \Phi_n \left(\int_{T^1_x} h_x \, d\chi(\boldsymbol{v}) \right) d\chi(x), \tag{5.3}$$

where Φ_n is the operator that replaces a function with its upper-continuous (for n even) or lower-continuous (for n odd) extension over 0-dimensional discontinuities.

Proof. The rationale: the inner integral has the effect of aggregating all targets visible at x during a complete sweep over the unit tangent sphere $T^1_x(\mathbb{R}^n) \cong S^{n-1}$. The outer integral would give $\sum_\alpha \chi(U_\alpha)$ in accordance with Theorem 2.6. We need to check for contractibility of the target supports for both integrals, and perform a modification (via Φ_n) in cases where this fails and a defect occurs.

Fix a value of x distinct from all targets. Because the sensing cone is convex and rotated by $\boldsymbol{v}$, the 'angular' support of each target $\mathcal{O}_\alpha$ is a convex (hence contractible) subset of T^1_x. Thus, the inner integral of Eqn. (5.3) yields the total number of targets visible from x after a full sweep of the tangent sphere. However, when x is at a target $\mathcal{O}_\alpha$, then $\mathcal{O}_\alpha$ is visible during the entire sweep, and its support in T^1_x is the entire $(n-1)$-dimensional sphere. This contributes an erroneous count of $1-(-1)^n$ to $\int h_x \, d\chi$. This, in turn, impacts the integral in Eqn. (5.3) and affects the enumeration of $|\mathcal{U}|$, over-counting for n odd and under-counting for n even. The operator Φ_n wipes out positive codimension defects. By the general position assumption, the defects caused by sensors on top of targets are the only such strata on which the integrand is modified. Thus Φ_n returns the correct height function for the workspace.

To finish the proof, we check that the target supports U_α are contractible. Choosing an $x \in U_\alpha$ means that $\mathcal{O}_\alpha \in C(x, \boldsymbol{v})$ for some bearing vector $\boldsymbol{v}$. Since the cones are uniform in x and $\boldsymbol{v}$, this implies that $y \in U_\alpha$ for all y on the line segment from x to $\mathcal{O}_\alpha$. Thus U_α is star-convex and, in particular, contractible. □

In the case of a network of sensors, one can assume that the sensors are not at the same location as the targets and the interpolations of §5.1 will hide these defects. However, in the case of continuous fields or in the (more realistic) case where the sensors' detection cones diffuse to a small neighborhood of the sensors, these holes in the height function need to be annealed away.

6. Discussion. The goal of this paper is to introduce integration with respect to Euler characteristic as a powerful and computable tool to perform target enumeration in networks of extremely weak sensors. As with all problems in sensor networks, the fundamental issue is the passage from local information to global information. This paper contributes to the thesis that topology is an ideal tool for managing the local-to-global transition.

This is an introductory paper to the mathematical techniques, and we have ignored many of the complications present in physical sensor networks and important to implementation. In particular, we have not dealt with communication and signal protocol issues, the difficulty of localizing nodes, and the stochastic nature of networks. We are optimistic that the surprising degree of robustness which these topological methods exhibit will be of assistance in many of these issues.

For the sake of simplicity, we have also not been comprehensive in either the methods available or in the possible applications. We outline a few possible extensions below in the form of a sequence of remarks and open questions.

REMARK 6.1. Throughout this article we have assumed that the appropriate support U_α associated to each target $\mathcal{O}_\alpha$ on which the target's presence is be sensed is a contractible set. There are instances, however, when such an assumption is invalid. One example comes from beacon visibility in robotic navigation systems. One such model for beacon navigation is that the node (robot) can see any beacon whose distance is within an interval bounded away from zero. The upper bound on distance is clear; the lower bound represents the fact that beacons which are too close cannot be seen. For a workspace $X = \mathbb{R}^n$, this assumption leads to supports with the topology of $S^{n-1} \times [0, 1]$. Ironically, in the most physical case $n = 2$, the supports are annuli with Euler characteristic zero, and the ensuing height function h always satisfies $\int h \, d\chi = 0$. However, for domains in $\mathbb{R}^3$, the solution is trivial: $|\mathcal{U}| = \frac{1}{2} \int h \, d\chi$.

REMARK 6.2. There are instances for which what is known is not the support U_α of each target, but rather the support of each sensor — the neighborhood of the sensor on which the target can be sensed (see, *e.g.*, Problem 5.6). It is often possible to infer the topology of the target support from that of the sensor support, as in the proof of Theorem 5.7. One simple example is in the case where X is a Euclidean domain and sensing is by line-of-sight. Then the support of each sensor is star-convex with respect to the sensor node and moving the sensor along the ray to the target never impairs visibility. Then the associated target support is likewise star-convex and thus contractible.

REMARK 6.3. The sensors used in this paper are extremely weak, with no range-finding, bearing, time-stamp, or other sophisticated capabilities. However, we do assume the ability to produce a local count of nearby targets (in Problem 1.1). A yet simpler sensor would be one which returns a value in $\{0, 1\}$ depending on whether it lies with the union of target supports or not. Estimating the number of targets in this setting will require much stronger assumptions about the sensor ranges and target supports, and will rely on results from discrete geometry.

REMARK 6.4. The enumeration problems of this paper lead to consideration of integrands

which are of the form $\sum_\alpha \mathbb{1}_{U_\alpha}$. There are similar enumeration problems for functions which are not of this precise form. For example, given a continuous real-valued distribution over a domain X, what is the minimal decomposition as a sum of unimodal functions over contractible supports? The techniques of this paper may be applicable.

REMARK 6.5. In this paper, the network sampling of points in X was assumed to be done on a grid of known geometry. In practice, an ad-hoc wireless network may be employed, in which case, knowledge of the appropriate grid or even of the node locations may be impossible. Likewise, in situations where the sensor nodes are mobile, one wants to determine a global count based on temporal sweeping. The recent work on homological methods for sensor networks [7] provides tools for addressing these issues.

REMARK 6.6. Since it is based on an integration theory, the enumeration of observables detailed in this paper obeys a subadditivity principle. To wit:

$$\int_{A\cup B} h\, d\chi = \int_A h\, d\chi + \int_B h\, d\chi - \int_{A\cap B} h\, d\chi.$$

Thus, enumeration can be performed in a distributed manner easily.

REMARK 6.7. For sensors which do more than a simple numerical count — *e.g.*, they can register logical statement about the observables in range — one wants a means to integrate these logical statements into a global deduction about the population. We believe that an integral approach is possible in these settings as well. The appropriate underlying perspective is that of sheaf theory, the impetus behind the mathematics of the present paper.

REFERENCES

[1] R. Adler, *The Geometry of Random Fields*, Wiley, 1981.
[2] R. Adler, "On excursion sets, tube formulas and maxima of random fields," *Ann. Appl. Probab.* 10, 2000, 1–74.
[3] W. Blaschke, *Vorlesungen über Integralgeometrie*, Berlin, 1955.
[4] A. Boulis, S. Ganeriwal, and M. Srivastava, "Aggregation in sensor networks: an energy - accuracy tradeoff," *J. Ad-hoc Networks*, 1, 2003, 317–331.
[5] L. Bröcker, "Euler integration and Euler multiplication," *Adv. Geom.* 5, 2005, 145–169.
[6] R. Cluckers and M. Edmundo, "Integration of positive constructible functions against Euler characteristic and dimension," *J. Pure Appl. Algebra*, 208, no. 2, 2006, 691–698.
[7] V. de Silva and R. Ghrist, "Coordinate-free coverage in sensor networks with controlled boundaries," *Intl. J. Robotics Research* 25(12), 2006, 1205–1222.
[8] D. Estrin, D. Culler, K. Pister, and G. Sukhatme, "Connecting the Physical World with Pervasive Networks," *IEEE Pervasive Computing* 1:1, 2002, 59–69.
[9] M. Goresky and R. MacPherson, *Stratified Morse Theory*, Springer-Verlag, 1988.
[10] H. Groemer, "Minkowski addition and mixed volumes," *Geom. Dedicata* 6, 1977, 141–163.
[11] L. Guibas. "Sensing, Tracking and Reasoning with Relations," *IEEE Signal Processing Magazine*, 19(2), Mar 2002, .
[12] H. Hadwiger, "Integralsätze im Konvexring," *Abh. Math. Sem. Hamburg*, 20, 1956, 136–154.
[13] T. He, P. Vicaire, T. Yan, L. Luo, L. Gu, G. Zhou, R. Stoleru, Q. Cao, J. Stankovic, T. Abdelzaher, "Achieving Real-Time Target Tracking UsingWireless Sensor Networks," in proceedings of *IEEE Real Time Technology and Applications Symposium*, 2006, 37–48.
[14] B. Jung and G. Sukhatme, "A Region-Based Approach for Cooperative Multi-Target Tracking in a Structured Environment," in proceedings of *IEEE/RSJ Conference on Intelligent Robots and Systems*, 2002.
[15] M. Kashiwara and P. Schapira, *Sheaves on Manifolds*, Springer-Verlag, 1994.
[16] D. Klain, K. Rybnikov, K. Daniels, B. Jones, C. Neacsu, "Estimation of Euler Characteristic from Point Data," preprint 2006.
[17] T. Kong and A. Rosenfeld (eds.) *Topological Algorithms for Digital Image Processing*, Elsevier, 1996.

[18] D. Li, K. Wong, Y. Hu, and A. Sayeed, "Detection, classification, and tracking of targets," *IEEE Signal Processing Magazine*, 19(2), 2002, 17–30.
[19] J. Milnor, *Morse Theory*, Princeton University Press, 1963.
[20] R. Morelli, "A Theory of Polyhedra," *Adv. Math.* 97, 1993, 1–73.
[21] P. Schapira, "Operations on constructible functions," *J. Pure Appl. Algebra* 72, 1991, 83–93.
[22] P. Schapira, "Tomography of constructible functions," in proceedings of *11th Intl. Symp. on Applied Algebra, Algebraic Algorithms and Error-Correcting Codes*, 1995, 427-435.
[23] A. Takemura and S. Kuriki, "On the equivalence of the tube and Euler characteristic methods for the distribution of the maximum of Gaussian fields over piecewise smooth domains," *Ann. Appl. Probab.* 12(2), 2002, 768–796.
[24] L. Van den Dries, *Tame Topology and O-Minimal Structures*, Cambridge University Press, 1998.
[25] O. Viro, "Some integral calculus based on Euler characteristic," Lecture Notes in Math., vol. 1346, Springer-Verlag, 1988, 127–138.
[26] K. Worsley, "Local Maxima and the Expected Euler Characteristic of Excursion Sets of χ^2, F and t Fields," *Advances in Applied Probability*, 26(1), 1994, 13–42.
[27] K. Worsley, "Estimating the number of peaks in a random field using the Hadwiger characteristic of excursion sets, with applications to medical images," *Ann. Statist.* 23, 1995, 640–669.
[28] J. Zhao, R. Govindan and D. Estrin, "Computing Aggregates for Monitoring Wireless Sensor Networks," in proceedings of *IEEE Intl. Workshop on Sensor Network Protocols and Applications (SNPA)*, 2003.